J Appl Electrochem (2007) 37:451–459
DOI 10.1007/s10800-006-9275-z

ORIGINAL PAPER

# Oxidation of herbicides by in situ synthesized hydrogen peroxide and fenton's reagent in an electrochemical flow reactor: study of the degradation of 2,4-dichlorophenoxyacetic acid

**Carla Badellino · Christiane Arruda Rodrigues · Rodnei Bertazzoli**

Received: 27 June 2006 / Accepted: 2 November 2006 / Published online: 30 January 2007


**Abstract** This paper reports an investigation of $H_2O_2$ electrogeneration in a flow electrochemical reactor with RVC cathode, and the optimization of the $O_2$ reduction rate relative to cell potential. A study of the simultaneous oxidation of the herbicide 2,4-dichlorophenoxyacetic acid (2,4-D) by the in situ electrogenerated $H_2O_2$ is also reported. Experiments were performed in 0.3 M $K_2SO_4$ at pH 10 and 2.5. Maximum hydrogen peroxide generation rate was reached at –1.6 V versus Pt for both acidic and alkaline solutions. Then, 100 mg $L^{-1}$ of 2,4-D was added to the solution. 2,4-D, its aromatic intermediates such as chlorophenols, chlororesorcinol and chlorinated quinone, as well as TOC were removed at different rates depending on pH, the use of UV radiation and addition of Fe(II). The acidic medium favored the hydroxylation reaction, and first order apparent rate constants for TOC removal ranged from $10^{-5}$ to $10^{-4}$ $s^{-1}$. In the presence of UV and iron, more than 90% of TOC was removed. This value indicates that some of the intermediates derived from 2,4-D decomposition remained in solution, mainly as more biodegradable light aliphatic compounds.

**Keywords** Hydrogen peroxide · Electrosynthesis · Electro-Fenton reagent · Oxygen reduction · 2,4-dichlorophenoxyacetic acid

C. Badellino · C. A. Rodrigues · R. Bertazzoli (✉)
Faculty of Mechanical Engineering, Department of Materials Engineering, The State University of Campinas, CP6122, 13083-970 Campinas, Sao Paulo, Brazil
e-mail: rbertazzoli@fem.unicamp.br

## 1 Introduction

In the last two decades, electrosynthesis of hydrogen peroxide has received considerable attention, and several papers have demonstrated that in situ electrogenerated $H_2O_2$ may also be successfully used for the treatment of aqueous effluents containing organic pollutants [1–13]. Hydrogen peroxide is a popular non-selective oxidizing reactant for the oxidation of organic pollutants to carbon dioxide. Its reactivity is determined largely by the ratio of the concentration of $H_2O_2$ to substrate, and by reaction conditions, particularly the presence of Fe ions and UV radiation, both of which increase the rate of hydroxyl radical formation. Furthermore, hydrogen peroxide reactions leave no residuals in the reaction stream. In concentrations such as those produced in electrolysis cells, its reactions are non-hazardous, and take place under moderate conditions. $H_2O_2$ electrosynthesis is also of interest because of the cost and risks associated with transportation, storage and handling of concentrated hydrogen peroxide. Graphite flat plates [1, 2] and three-dimensional electrodes made from reticulated vitreous carbon (RVC) [3–6], and gas diffusion electrodes (GDE) [7–13] have been used to reduce oxygen to hydrogen peroxide. This paper reports an investigation of the performance of an electrochemical flow reactor, using a RVC cathode for $H_2O_2$ electrosynthesis and the simultaneous oxidation of the herbicide 2,4-dichlorophenoxyacetic acid (2,4-D).

The choice of RVC for the porous cathode is based on the observation that this material: (a) is chemically and electrochemically inert over a wide range of potentials and with a broad variety of chemicals; (b) has a high specific surface area within

the porous structure that is accessible to electrochemically active species; (c) has a high fluid permeability; and (d) is easily shaped as required by cell design considerations. Furthermore, vitreous carbon has good selectivity for hydrogen peroxide electrosynthesis. The oxygen reduction overall reaction is a four-electron reaction, and hydrogen peroxide is formed after the transfer of the first two electrons. On vitreous carbon the formation of hydrogen peroxide and its oxidation to water are separated by 400 mV [14].

The substance chosen for this study, 2,4-D, is an aryloxoalkanoic acid, and works as a systemic herbicide to control many types of broadleaf weeds. Human exposure occurs through agricultural use, food products, or lawn and garden use. Continuous use may cause soil percolation and groundwater contamination. Effects of exposure of professional applicators, homeowners and bystanders have been studied, but the risk of 2,4-D to human health has not been completely assessed [15]. However, the central nervous system is a target organ for the effects of this herbicide in different animal species [16]. Due to the refractory nature of 2,4-D to degradation, an increasing interest in alternative processes for its oxidation has been registered in the literature. Advanced oxidation processes using titanium dioxide [17] and zinc oxide [18] as photocatalysts have been reported, and the yield of 2,4-D degradation is dependent on the mass of semiconductor, temperature, and solution pH. Nevertheless, the measured TOC values remained constant during illumination, indicating that mineralization hardly occurs. Ozonation, in the presence of UV light and catalysed by iron ions, has shown a high efficiency for the degradation of 2,4-D, its aromatic intermediates and organic acids. Hydrogen peroxide and Fenton's reagent, both under UV radiation, have also shown higher conversion rates to carbon dioxide [19–21].

Degradation of 2,4-D by the attack of hydroxyl radicals has been investigated, and the motivation for these studies is due mainly to the refractory nature of the 2,4-D to oxidation. Resulting intermediates of 2,4-D hydroxylation are chlorophenols, chlororesorcinol and chlorinated quinone [6, 22, 23]; total mineralization hardly occurs [6].

This paper presents a two-step study for (i) the optimization of hydrogen peroxide electrogeneration rate related to cell potential and oxygen feed rate, and (ii) investigation of the kinetics of 2,4-D degradation by in situ electrogeneration of hydrogen peroxide and Fenton's reagent.

## 2 Experimental details

### 2.1 Apparatus and procedures

Figure 1 presents an expanded view of the divided flow-through cell reactor. The cathode central plate (A) is a 304 AISI stainless steel current feeder in a PP frame (135 mm × 310 mm × 1.5 mm), onto which 80 ppi RVC (50 mm × 150 mm × 6 mm) plates were bonded on both sides with thermally curable Dylon PX Grade Graphpoxy conducting epoxy. Anolyte and catholyte flows were separated by a N424 Nafion® membrane (B), and both anodes (C) were 1.5 mm thick titanium plates coated with $(Ta_2O_5)_{0.6}(IrO_2)_{0.4}$, marketed as DSA-$O_2^{®}$ and supplied by De Nora do Brasil Ltd. Total geometric anodic area was 150 $cm^2$. End plates (D) were made from 15 mm thick PP. Between each plate and membranes, a rubber gasket was used to prevent leakage. Taking into account the thickness of rubber gaskets and membrane, the interelectrode gap was 5 mm. The recirculation system comprised flow meters, pumps and 3.5 L reservoirs. During the experiments the electrochemical reactor was operated in batch recirculation mode at a flow rate of 300 L $h^{-1}$, corresponding to a linear velocity of 0.07 m $s^{-1}$. Calculation of solution velocity considered that RVC has a voidage of 93%.

A platinum tip, inserted between the membrane and the RVC cathode, was used as a pseudo-reference electrode. By using Pt as reference, a potential shift of 0.7 V more negative was observed when compared to potentials referred to SCE. All experiments were controlled by an Autolab potentiostat/galvanostat PGSTAT 20. To prevent solution heating and improve oxygen solubility, the temperature was kept at 10°C, in line with previous experiments [6, 15]. A ¼'' 304 AISI stainless steel cooling coil was inserted into the catholyte reservoir and filled with a recirculating 25% ethylene glycol solution. In the experiments in which

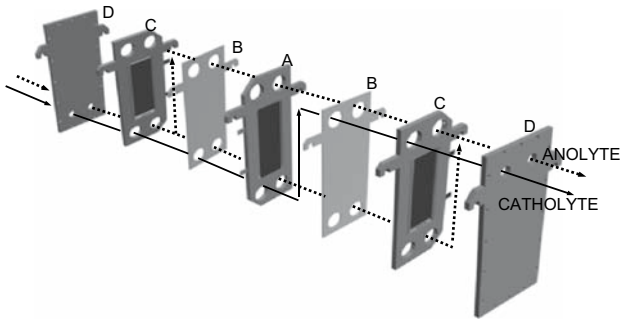


**Fig. 1** Expanded view of the electrochemical reactor

$H_2O_2$ oxidizing action was accelerated by UV radiation, an 8 W Sankyo Denki G8T5 germicidal lamp (fluency rate 31.1 J $m^2$ $s^{-1}$ and $\lambda_{max}$ = 254 nm) was inserted into the catholyte reservoir.

Experiments reported here were basically conducted at constant potential. Controlled potential electrolysis was used for the optimization of $H_2O_2$ electrogeneration rate related to potential oxygen flow rate. During electrolysis of $O_2$ saturated solutions, the catholyte was sampled at pre-determined time intervals and $H_2O_2$ concentration was measured. Then, the $H_2O_2$ electrogeneration rate was obtained as a function of potential in the range of –1.4 V–1.7 V versus Pt. Once the process was optimized the pesticide was added to the supporting electrolyte and its degradation was followed by HPLC.

### 2.2 Solutions

Supporting electrolyte was always $K_2SO_4$ 0.3 M, and NaOH or $H_2SO_4$ were added to adjust the pH to 10 or 2.5, respectively. For the electrolysis carried out in acidic medium, pH was mantained by continuous dripping of $H_2SO_4$ solution. Oxygen was bubbled into the catholyte. At flow rates of 6 and 8 L $min^{-1}$ the resulting oxygen concentration, measured by an Orion DO sensor, was 25 mg $L^{-1}$ (0.78 mmol $L^{-1}$). Analytical grade Aldrich 2,4-D was used as received, and 100 mg $L^{-1}$ was added to the supporting electrolyte for the experiments. After 2,4-D addition, the solution had a TOC value of about 50 mg $L^{-1}$. When needed, 1 mM of $FeSO_4$ was added to the solution to achieve Fenton's reagent composition. The volume of solution used for all experiments was 3.5 L.

### 2.3 Analytical control

Hydrogen peroxide concentration was determined by potentiometric titration using a standardized $KMnO_4$ 0.01 N solution in an automatic 702SM Metrohm titrator. 2,4-D degradation was followed by a Shimadzu HPLC instrument, with a Supelco LC–18 reversal phase column, 5 μm × 4.6 mm × 250 mm, and $H_2O$/$CH_3CN$/$CH_3COOH$, 52:46:2 (%/%) mobile phase. The UV detector was set at 280 nm and the flow rate was 1.2 mL $min^{-1}$. Formation and degradation of 2,4-D intermediates were also followed by HPLC. Analytical grade 2,4-D (Aldrich) was used to establish a calibration curve in the concentration range 0–100 mg $L^{-1}$ for 2,4-D. Similar calibration curves were obatined in the concentration range 0–50 mg $L^{-1}$ for the intermediates 2,4-dichlorophenol (2,4-DCP), 2,4-dichlororesorcinol (2,4-DCR), 4,6-dichlororesorcinol (4,6-DCR), 2-chlorohydroquinone (2-CHQ) and 2-chlorobenzoquinone (2-CBQ), all purchased from Aldrich.

Total organic carbon (TOC) values were obtained in a TOC 5000 Shimadzu equipment.

## 3 Results and discussion

### 3.1 Optimization of $H_2O_2$ electrosynthesis

Experiments for the optimization of the generation rate of hydrogen peroxide in alkaline medium were conducted using a 0.3 M $K_2SO_4$ solution with pH 10, in which $O_2$ was bubbled into the catholyte reservoir throughout the electrolysis time. Based on previous voltammetric experiments [6], the potential was ranged from –1.4 V to –1.7 V versus Pt and the solution was recirculated at 300 L $h^{-1}$ (0.07 m $s^{-1}$). Figure 2 shows curves of hydrogen peroxide concentration as a function of electrolysis time obtained at a temperature of 10°C. Up to a potential of –1.6 V, $H_2O_2$ formation rate increased with applied potential and concentration increased continuously during the time scale of the experiment. For –1.7 V the hydrogen peroxide generation rate decreased, indicating that higher overpotential values favoured water formation, or the reduction of $O_2$ directly to $H_2O$ in a four electron exchange reaction. Figure 2 also shows the current behaviour during electrolysis.

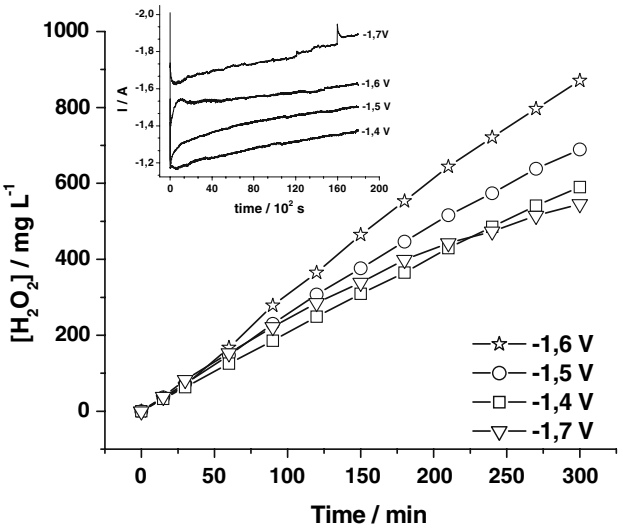


**Fig. 2** $H_2O_2$ concentration profiles as a function of electrolysis time for the potentials as shown. Inset: current values during electrolysis. Solution: 3.5 L of $K_2SO_4$ 0.3 M, pH 10. $O_2$ flow rate of 0.1 L $s^{-1}$

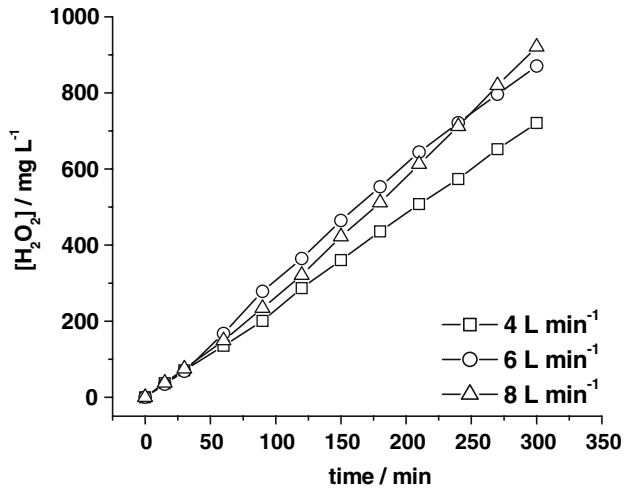


**Fig. 3** $H_2O_2$ concentration profiles as a function of electrolysis time for the oxygen flow rates as shown. Solution: 3.5 L of $K_2SO_4$ 0.3 M, pH 10. Potential of –1.6 V versus Pt

Oxygen flow rate also plays an important role in the electrosynthesis of hydrogen peroxide. Figure 3 shows curves of hydrogen peroxide concentration as a function of oxygen flow rate. In the flow rate range chosen for the experiments, from 0.07 L $s^{-1}$ to 0.1 L $s^{-1}$, an increase in formation rate is observed. However, at a flow rate of 0.13 L $s^{-1}$ no substantial improvement in the amount of hydrogen peroxide formed was observed. In the conditions of recirculation flow rate and temperature of the experiments, a value of 0.1 L $s^{-1}$ is probably sufficient for the solution saturation; furthermore, when 0.13 L $s^{-1}$ was used, two-phase flow was observed.

It is worth noting that the oxygen reduction reaction is not mass transfer limited in the operating conditions reported here. Apparently, currents resulting from the controlled potential experiments are below the limiting current and dissolved oxygen is still in excess. As a consequence hydrogen peroxide synthesis followed pseudo-zero order kinetics as can be seen in Fig. 2 and 3. By running the electrolysis at 300 L $h^{-1}$, at a temperature of 10°C, at the optimal conditions of –1.6 V and oxygen flow rate of 0.1 L $s^{-1}$, calculations showed that the apparent rate constant for hydrogen peroxide formation had an average value of $5 \times 10^{-5}$ g $L^{-1}$ $s^{-1}$, or $6.7 \times 10^{-2}$ g $L^{-1}$ $m^{-2}$ $s^{-1}$ considering the geometric electrode area. Within 5 h of electrolysis the concentration reached 0.9 g $L^{-1}$. In an attempt to run electrolysis in such conditions that oxygen reduction reaction is mass transfer limited, a higher value of potential, –1.7 V, was used. Figure 2 shows that at this potential performance is poor, due to an increase in the water formation rate and a drop in the $H_2O_2$ apparent rate constant to $4.8 \times 10^{-2}$ g $L^{-1}$ $m^{-2}$ $s^{-1}$.

By operating the electrolysis in conditions of mixed control, a current efficiency lower than 100% at –1.6 V and below was observed. Probable reasons for such a low current efficiency are simultaneous water formation and hydrogen peroxide decomposition. For potentials up to –1.6 V, a constant current efficiency of 65% was observed. At –1.7 V this dropped to less than 40%. Energy consumption in the optimal condition is 34.7 kWh $kg^{-1}$ of hydrogen peroxide.

The values found in the electrosynthesis of hydrogen peroxide for alkaline media can be extended to acidic media. When the solution pH is changed from 10 to 2.5 there is no appreciable increase in reaction rate and –1.6 V and oxygen flow rate of 0.1 L $s^{-1}$ are still optimal conditions to run the electrolysis. However, with electrolysis at pH 2.5, continuous pH control by $H_2SO_4$ solution dripping is required. Indeed, a tendency for the pH to increase is observed during electrolysis due to proton consumption in the oxygen reduction reaction according to Eq. 1.

$$O_2 + 2H^+ + 2e^- \rightarrow H_2O_2 \quad (1)$$

### 3.2 Experiments of 2,4-D degradation

Considering the results reported so far, the experiments for the degradation of 2,4-D were conducted at –1.6 V, 0.1 L $s^{-1}$ of oxygen, solution recirculation at 300 L $h^{-1}$ and a temperature of 10°C for both alkaline (pH 10) and acidic (pH 2.5) media. In the new series of experiments 100 mg $L^{-1}$ of the pesticide were added to the 0.3 M $K_2SO_4$ supporting electrolyte for the in situ generation of hydrogen peroxide and simultaneous hydroxilation of the pesticide. The generation of hydrogen peroxide is an electrochemical reduction process and 2,4-D, the compound chosen for this work, does not itself undergo degradation by reduction; this has already been reported in other studies [6]. For both alkaline and acidic media, 2,4-D either reacted simply with $H_2O_2$ ($H_2O_2$ process) or in the presence of UV radiation ($H_2O_2$/UV process). In acidic medium, another two processes were also used: with Fe(II) (electro-Fenton process), and $H_2O_2$ with Fe(II) accelerated by UV radiation (photoelectro-Fenton process).

Performances of all these processes are compared in Fig. 4, where profiles of the pesticide normalized concentration decay are shown as a function of electrolysis time. At pH 10 almost no degradation was observed for the $H_2O_2$ process due to the high stability of hydrogen peroxide at that pH [1]. However, by accelerating $H_2O_2$ decomposition with UV radiation ($H_2O_2$/UV process), the 2,4-D concentration drops exponentially, and the compound pratically disappears after 3 h. As

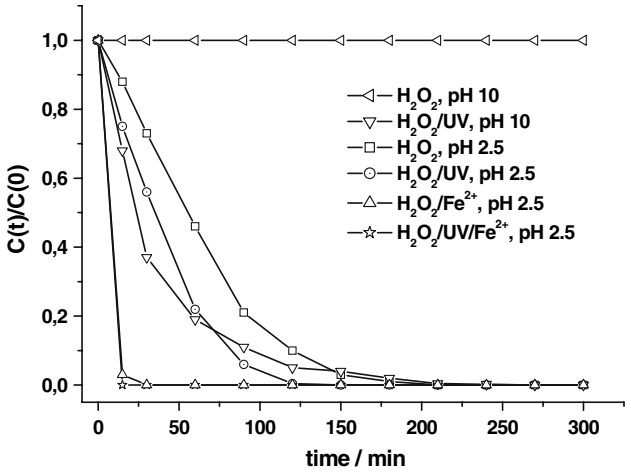


**Fig. 4** Normalized 2,4-D concentration decay as a function of electrolysis time for the processes as shown. Solution: 3.5 L of $K_2SO_4$ 0.3 M, pH 10. $O_2$ flow rate of 0.1 L $s^{-1}$

will be seen later, this does not mean simultaneous oxidation of intermediates or mineralization. In acidic medium the performance is better. The $H_2O_2$ process and $H_2O_2$/UV process reduced the 2,4-D concentration satisfactorily. However, in the presence of Fe(II), a superior performance was observed for both the electro-Fenton and the photoelectro-Fenton process.

The ability of hydrogen peroxide to oxidize an organic substrate (R) is due to the reaction:

$$H_2O_2 + R \rightarrow RO + H_2O \quad (2)$$

Intermediates of the hydrogen peroxide decomposition, such as the peroxide anion and hydroxyl radicals, are responsible for the organic oxidation. However, when stimulated by UV radiation, the rate of hydrogen peroxide decomposition into hydroxyl radicals ($OH^{\bullet}$) increases, which explains the superior performance exhibited by the $H_2O_2$/UV process. UV-catalysed decomposition of hydrogen peroxide is represented by Eq. 3.

$$H_2O_2 \xrightarrow{h\nu} 2OH^{\cdot} \quad (3)$$

Thus, hydroxyl radicals are responsible for the combustion of the organic compound as follows:

$$R + OH^{\cdot} \rightarrow CO_2 + H^+ + e^- \quad (4)$$

With Fe(II) in solution, the high performance is also due to an increase in the decomposition rate of $H_2O_2$ into $OH^{\bullet}$ according to:

$$Fe^{2+} + H_2O_2 \rightarrow Fe^{3+} + OH^- + OH^{\cdot} \quad (5)$$

Then, Fe(III) is reduced to Fe(II) by both electron transfer at the cathode surface and photo-reduction, thus regenerating Fentoń s reagent according to:

$$Fe^{3+} + e^- \rightarrow Fe^{2+} \quad (6)$$

$$[Fe(OH)]^{2+} + h\nu \rightarrow Fe^{2+} + OH^{\cdot} \quad (7)$$

By examining both curves from Fig. 4 of 2,4-D concentration decay in the presence of iron (electro-Fenton and photoelectron-Fenton processes) there is no noticeable difference in the hydroxylation rate. However, synergism between reactions represented by equations 5 and 6 will become clearer by examining TOC behavior later on. Furthermore, during the removal of 2,4-D from solution by hydroxyl radical attack, $H_2O_2$ is still being generated and consumed. Indeed, $H_2O_2$ is consumed at very different rates as can be seen in Fig. 5. This figure compares $H_2O_2$ remaining concentration profiles in the presence of the substrate being oxidized during the electrolysis time for the processes under consideration. Results depicted in Fig. 5 corroborate those of Fig. 4. When the 2,4-D removal process is less efficient, more $H_2O_2$ remains in solution ($H_2O_2$ and $H_2O_2$/UV processes in alkaline solution). For the processes with a higher 2,4-D removal rate only residuals of $H_2O_2$ can be measured in the course of electrolysis; the remaining concentration oscillates in the range from a non-detectable value to 50 mg $L^{-1}$.

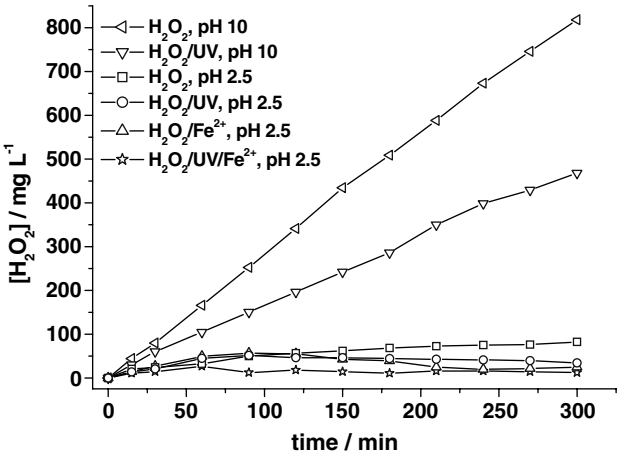


**Fig. 5** Remaining concentration of hydrogen peroxide during simultaneous hydroxylation of 2,4-D for the process as shown

### 3.3 Evolution of concentration of 2,4-D intermediates

The main aromatic intermediates resulting from the oxidation of 2,4-D were previously identified by GC-MS [6, 17, 18]. Then, the pesticide intermediate concentrations were followed by HPLC according to the procedure described in the Experimental Section. Considering the best performance in acidic medium, only samples processed at pH 2.5 were analysed. Figure 6(A–D) shows some of the chromatograms obtained during electrolysis for the $H_2O_2$ process. Peak 1 (retention time of 7.7 min), which decreases rapidly, is related to 2,4-D, and peak 2, at 8.8 min is a result of

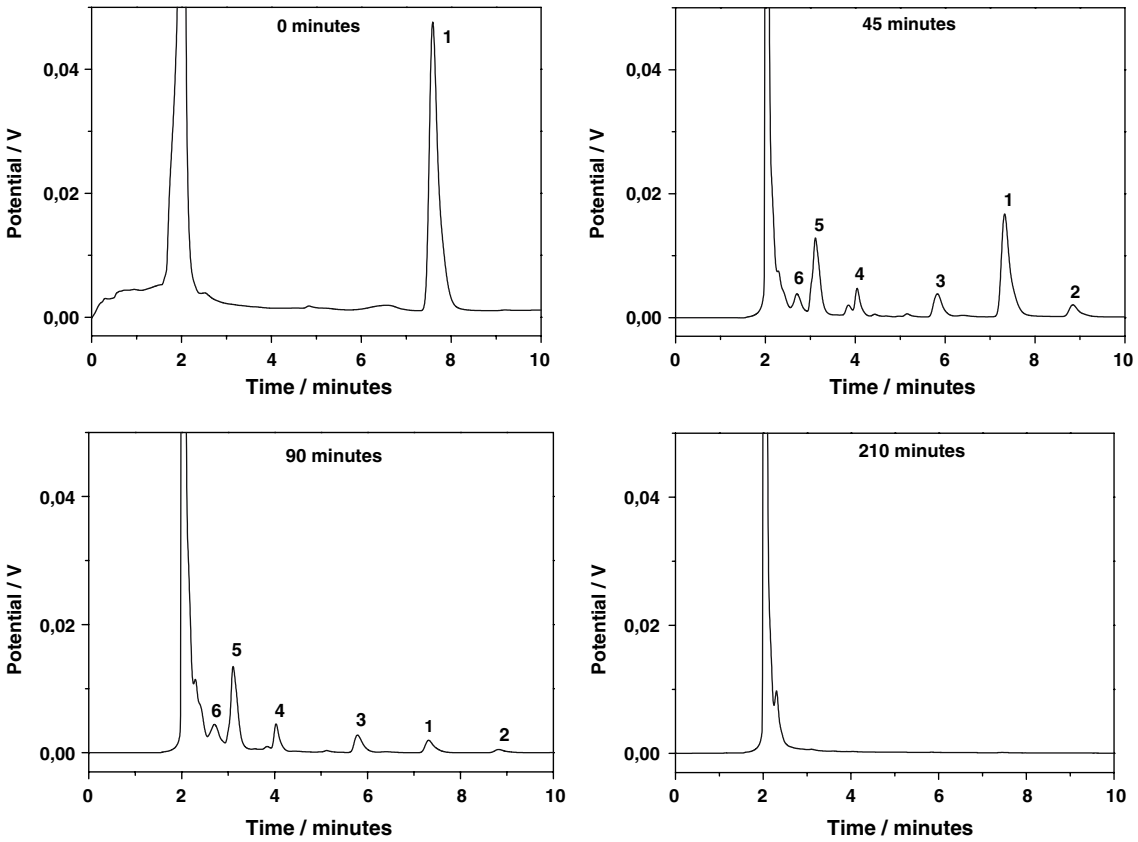


**Fig. 6** Evolution of 2,4-D intermediates during electrolysis shown by HPLC chromatograms for samples taken at (**A**) 0 min, (**B**) 45 min, (**C**) 90 min, and (**D**) 180 min. $H_2O_2$ process, pH 2.5, without catalysts

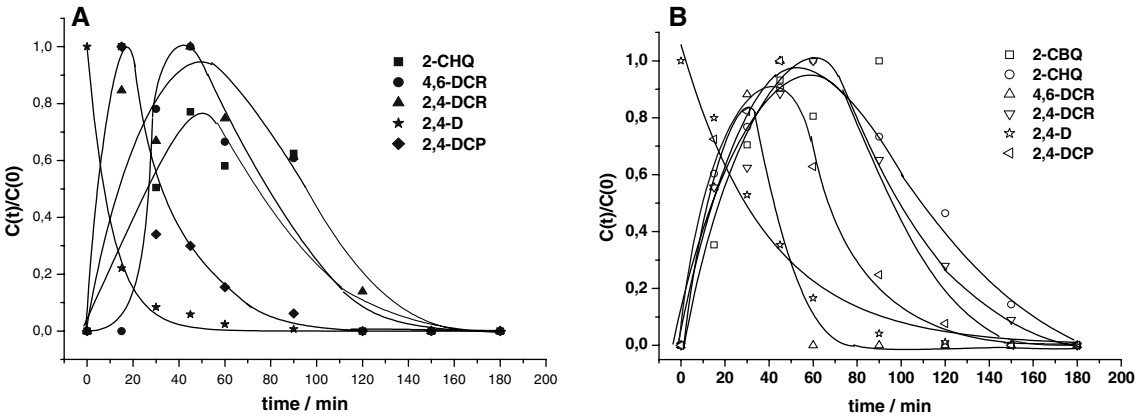


**Fig. 7** Evolution of normalized 2,4-D intermediates concentration during electrolysis for $H_2O_2$ process (**A**) and $H_2O_2$/UV process (**B**), both at pH 2.5

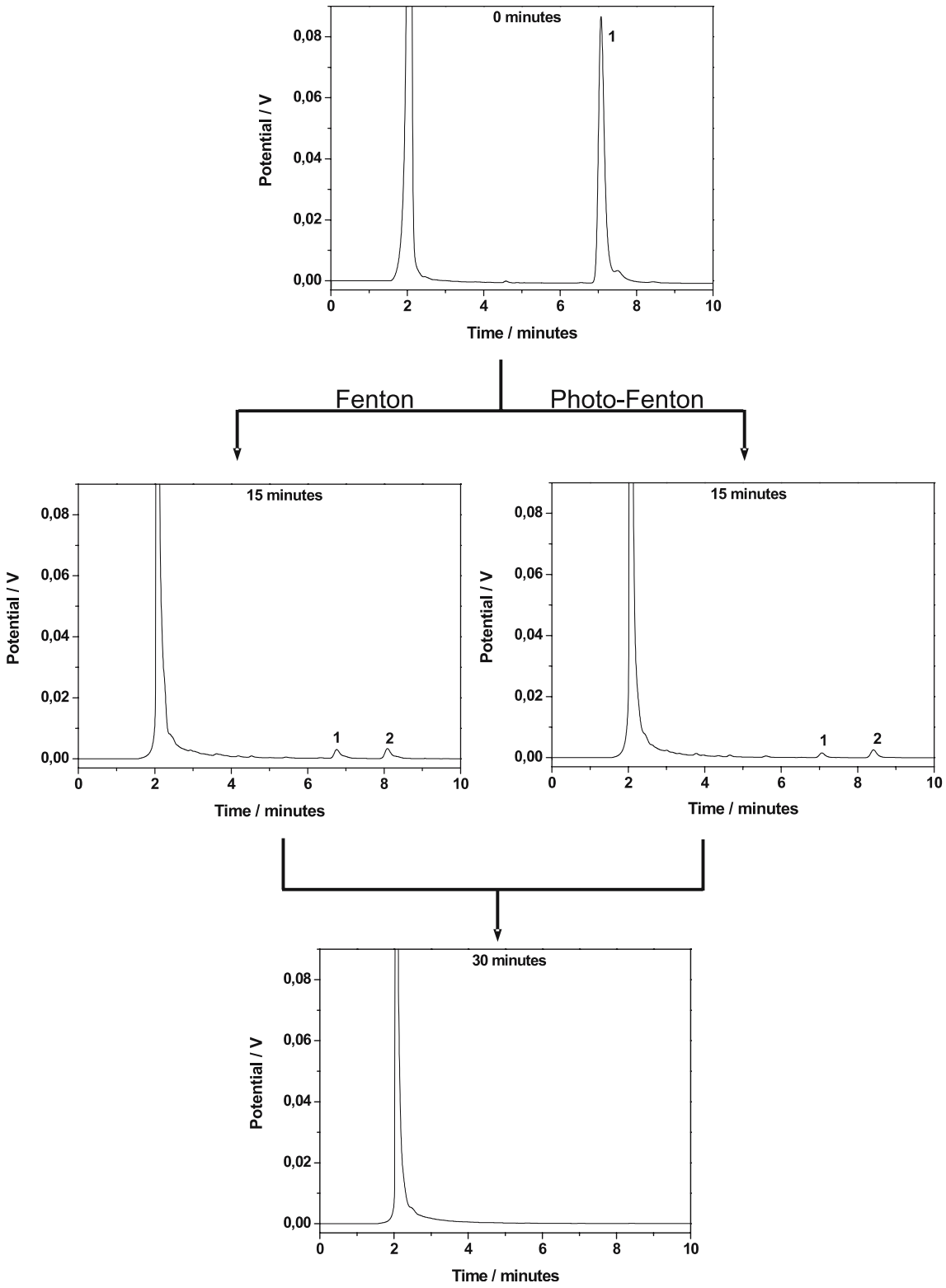


**Fig. 8** Evolution of 2,4-D intermediates during electrolysis shown by HPLC chromatograms for samples taken at 0 min, 15 min, and 30 min, for the electro-Fenton and photoelectron-Fenton processes, pH 2.5

the first attack by hydroxyl radicals in which 2,4-dichlorophenol (2,4-DCP) is formed. Other hydroxylated derivatives can be observed at peaks 3 (retention time of 5.8 min) and 4 (retention time of 4.0 min) which are 2,4-dichlororesorcinol (2,4-DCR) and 4,6-dichlororesorcinol (4,6-DCR), respectively. Peak 5, at 3.1 min,

represents the early stages of dechlorination and the formation of 2-chlorohydroquinone (2-CHQ), and peak 6 (2.7 min) corresponds to the formation of 2-chlorobenzoquinone (2-CBQ). They are the main, but not the only, intermediates formed during the 2,4-D hydroxylation reaction as can be seen by superimposition of peaks, as in the peak 4.

Figure 7A shows the simultaneous evolution of the normalized concentration of 2,4-D derivatives including other samples not shown in Fig. 6. No aromatic derivatives remain in the solution after three hours electrolysis. This is not an indication of mineralization, since aliphatic compounds may still be in solution. Indeed, less 20% than TOC concentration was reduced in this experiment. However, results reported so far are an indication of good performance in aromatic ring opening and of improvement in pollutant biodegradability.

By stimulating hydrogen peroxide decomposition with UV radiation the time demanded for degradation of aromatic intermediates was reduced. Figure 7B shows that most of the identified intermediates disappeared within 150 min. Even considering that the gain in the electrolysis time is not noticeable in comparison to the non-UV process, reduction of TOC concentration was 40% in 180 min. This is an indication of simultaneous ring opening and mineralization to a greater extent. Hydroxyl radicals, formed according to Eq. 3, are responsible for the combustion of the organic compounds.

Finally, the addition of Fe(II) to the solution has substantially improved the process performance as a whole. Time demanded for aromatic intermediate disappearance was greatly reduced, and TOC concentration decay was faster. Less than thirty minutes of electrolysis were enough for the degradation of the aromatic intermediates, as can be seen in Fig. 8.

### 3.4 Conversion of 2,4-D to carbon dioxide

By extending the electrolysis time to over 300 min, a substantial TOC reduction is observed. Figure 9 compares TOC reduction for the four processes considered here. As already said, TOC concentration decayed by 20 and 40% for the $H_2O_2$ and $H_2O_2$/UV processes, respectively, in 180 min. With Fe(II) in solution 55% of TOC is eliminated for the electro-Fenton process and 75% for the photoelectron-Fenton process in the same period. Curves depicted in Fig. 9 show a near exponential decay suggesting a pseudo-first order kinetics. Calculations of rate constants for TOC reduction gives $2.5 \times 10^{-5}\ s^{-1}$ ($H_2O_2$ process), $6.8 \times 10^{-5}\ s^{-1}$ ($H_2O_2$/UV process), $9.4 \times 10^{-5}\ s^{-1}$ ($H_2O_2$/Fe(II) process) and $1.7 \times 10^{-4}\ s^{-1}$($H_2O_2$/UV/Fe(II) process). According to the results discussed so far a difference between electro-Fenton and photoelectron-Fenton processes appeared only when TOC reduction is considered. A greater degree of combustion of organics is observed for the latter process. Although electron transfer at the cathode surface is responsible for the iron cycle (see Eqs. 5 and 6), photo-reduction of Fe(III) also plays an important role in Fenton's reagent regeneration (see Eq. 7). Furthermore, the superior performance shown by the photoelectron-Fenton process can also be explained by the photodecarboxilation of the complexes of Fe(III) with carboxilic acids as already observed [17], which explains the higher degree of mineralization.

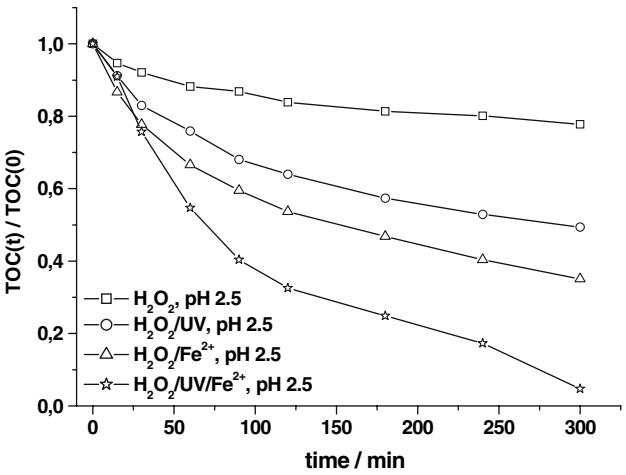


**Fig. 9** TOC concentration decay as a function of electrolysis time for the processes as shown

## 4 Conclusions

Electrogeneration of hydrogen peroxide by oxygen reduction is an efficient means of controlling organic pollutant concentration in aqueous media. By using a divided flow-through electrochemical reactor with a RVC cathode maximum generation rate was reached at –1.6 V versus Pt, in which the apparent rate constant for hydrogen peroxide formation was $5 \times 10^{-5}$ g $L^{-1}$ $s^{-1}$ and a concentration of 0.9 g $L^{-1}$ was reached after 5 h electrolysis. The apparatus was versatile and permitted the use of UV radiation and Fe(II). The processes were very effective for 2,4-D removal and its aromatic intermediates were also degraded. TOC reduction was favoured in acidic medium and in the presence of iron and UV radiation. Even considering the iron reduction on the electrode surface, UV radiation also played a

role in the iron cycle and in the regeneration of Fenton's reagent.

## References


1. Do J-S, Chen C-P (1993) J Electrochem Soc 140:1632
2. Do J-S, Chen C-P (1994) J Appl Electrochem 24:936
3. De-Leon CP, Pletcher D (1995) J Appl Electrochem 25:307
4. Alvarez-Gallegos A, Pletcher D (1998) Electrochim Acta 44:853
5. Alvarez-Gallegos A, Pletcher D (1999) Electrochim Acta 44:2483
6. Badellino C, Rodrigues CA, Bertazzoli R (2006) J Hazard Mat B137:856
7. Brillas E, Bastida R.M., Llosa E., Casado J (1995) J Electrochem Soc 142:1733
8. Brillas E, Mur E, Casado J (1996) J Electrochem Soc 143:L49
9. Brillas E, Saudela R, Casado J (1997) J Electrochem Soc 144:2374
10. Brillas E, Mur E, Saudela R, Sanches L (1998) Appl Catal B-Environ 16:31
11. Harrington T, Pletcher D (1999) J Electrochem Soc 146:2983
12. Brillas E, Banos MA, Camps S, Arias C, Cabot PL, Garrido JA, Rodriguez RM (2004) New J Chem 28:314
13. Brillas E,Cabot PL, Rodriguez RA, Arias C, Garrido JA Oliver R (2004) Appl Catal B- Environ 51:117
14. Rodrigues CA, Di-Iglia RA, Bertazzoli R (2001) Quimica Nova 24:252
15. Harris SA, Salomon KR, Stephenson GR (1992) J Environ Sci Health B 27:23
16. Bortolozzi AA, Duffard AME, Duffard R, Antonelli MC (2004) Neurotoxicol Teratol 26:599
17. Trillas M, Peral J, Doménech X (1995) Appl Catal B Environ 5:377
18. Sanches L, Peral J, Doménech X (1996) Electrochim Acta 41:1981
19. Pignatello JJ (1992) Environ Sci Technol 26:944
20. Sun YF, Pignatello JJ (1992) J Agricult Food Chem 40:322
21. Kwan CY, Chu W (2004) Water Sci Technol 49:117
22. Brillas E, Calpe JC, Casado J (2000) Water Res 34:2253
23. Oturan MA (2000) J Appl Electrochem 30:475